Electron cloud effects in intense, ion beam linacs theory and experimental planning for HIF

A. W. Molvik,* R. H. Cohen,† S. M. Lund,† F.M. Bieniosek,‡
E.P. Lee,‡ L.R. Prost,‡ P.A. Seidl,‡ and Jean-Luc Vay‡
Heavy-Ion Fusion Virtual National Laboratory

(Dated: May 21, 2002)

Abstract

Heavy-ion accelerators for HIF will operate at high aperture-fill factors with high beam current and long pulses. This will lead to beam ions impacting walls: liberating gas molecules and secondary electrons. Without special preparation a large fractional electron population ($\geq$1%) is predicted in the High-Current Experiment (HCX), but wall conditioning and other mitigation techniques should result in substantial reduction. Theory and particle-in-cell simulations suggest that electrons, from ionization of residual and desorbed gas and secondary electrons from vacuum walls, will be radially trapped in the $\sim$4 kV ion beam potential. Trapped electrons can modify the beam space charge, vacuum pressure, ion transport dynamics, and halo generation, and can potentially cause ion-electron instabilities. Within quadrupole (and dipole) magnets, the longitudinal electron flow is limited to drift velocities ($E \times B$ and ∇B) and the electron density can vary azimuthally, radially, and longitudinally. These variations can cause centroid misalignment, emittance growth and halo growth. Diagnostics are being developed to measure the energy and flux of electrons and gas evolved from walls, and the net charge and gas density within magnetic quadrupoles, as well as the their effect on the ion beam.

*molvik1@llnl.gov; Lawrence Livermore National Laboratory, Livermore, CA 945500, USA
†Lawrence Livermore National Laboratory, Livermore, CA 945500, USA
‡Ernest Orlando Lawrence Berkeley National Laboratory, 1 Cyclotron Road, Berkeley, CA 94720, USA

I. INTRODUCTION

Electron clouds have limited the performance of many positive-charge beam rings [1, 2]. We have initiated a program to determine whether they can also be dangerous in a linac. Three reasons for concern for heavy-ion fusion (HIF) induction linacs are: HIF injectors produce beams with line charges of $\sim$0.2 μCoul/m, resulting in several kilovolt beam potentials which can strongly confine electrons; injected pulses have a flattop duration of $\sim$20 μs which allows time for gas desorbed from walls to reach the beam; and HIF has an economic incentive to minimize induction-core mass by fitting beam tubes tightly to the beams; how tightly may be limited by the increased generation of gas and electrons from ion bombardment of walls and reduced time for these to reach the beam. Reducing the core mass is beneficial because the total in an inertial fusion power plant is predicted to be in the range of 10-30 $\times$ 10^6 kg, making it a major cost area [3]. Innovation is important for HIF, so the beam parameters listed in this paper are expected to evolve.

The present HIF experiments use potassium ion beams at energies of 0.5-1.8 MeV. The High-Curent Experiment (HCX) is studying coasting K^+ beams injected with 0.2-0.5 A at 1.0-1.8 MeV [4, 5]. The peak beam potential will range from 2 to 4.5 kV, and the flattop duration is 4 μs, with rise and fall times $\sim$1 μs. The HCX range of energies, 25-45 keV/nucleon, is near the peak cross section for ionization of background gas. Ionization of gas is expected to be the dominant electron source. (The maximum energy needed at the target in a power plant is in the range of 10-20 MeV/nucleon [6], where the cross sections are two orders of magnitude below the peak.) In the future we expect to perform electron experiments in the STS-500 which has pulse durations near 20 μs, as in the injector for a driver.

II. THEORY - INITIAL RESULTS

We have studied the confinement of electrons by positive potential particle beams primarily within a series of quadrupole magnets. Electron confinement by a beam in quadrupole magnets is similar to that in our previous studies of electron confinement by magnetic-mirror confined, hot-ion plasmas [7, 8]. The electron particle balance has two main contributions, electrons from ionization of neutrals that are born electrostatically trapped and electrons

from the wall, due to ion and photon impingement, that are born untrapped.

Electrons in a magnetic field have a conserved magnetic moment if they have a gyroradius which is small compared with the gradient scale length of the magnetic field. The magnetic moment is $\mu = v_\perp^2/2B$ where $v_\perp$ is the electron velocity perpendicular to the magnetic field B. As a result, electrons which have large pitch angles and/or low energies at the minimum-field-strength point along a field line are confined by the combination of electrostatic and magnetic fields.

This picture is only approximately correct, as electrons in a quadrupole magnetic field undergo jumps in the magnetic moment. These are negligible for field lines far from the axis. But untrapped electrons that pass moderately close to the axis can get trapped by this process and remain so for up to several hundred bounce times, $\sim$1 μs.

Electrons generated within the beam by ionization of gas are born trapped, and accumulate until the end of the beam pulse. This process, in conjunction with gas released from walls by ion impact, is expected to lead to a significant electron density. We expect that untrapped, secondary electrons from the wall, with trapping only from jumps in magnetic moment near the quadrupole-field nulls, will not build up to sufficiently high densities to significantly impact beam performance. However, if electron-electron instabilities reach significant levels, they could cause much greater trapping of secondary electrons.

The details of the electron transport differ between drift and magnetic quadrupole field regions. For a flattopped beam within a drift region, we expect the electron density to equilibrate axially, and azimuthally. Radially, electrons will be confined within the birth radius. Within a quadrupole magnet, electron transport is limited to the sum of the ∇B and $E \times B$ drift velocities, directed parallel or antiparallel to the beam, depending on the quadrupole quadrant. The drift velocities are a fraction of the beam directed velocity in HCX, requiring a fraction of a microsecond to drift the 31 cm length of a quadrupole magnet.

Electrons reaching a drift region rapidly free-stream to the next magnet where they either bounce back, or enter the next magnet, depending on the local drift velocity direction of that magnet. Those that bounce back to the first magnet continue to bounce until they drift azimuthally to where one of the magnets will accept them. Axial transport of electrons through a series of magnets during the flattop beam duration of 4 μs could be treated as a diffusion process.

This situation is significantly changed by an acceleration gap within a drift region. It

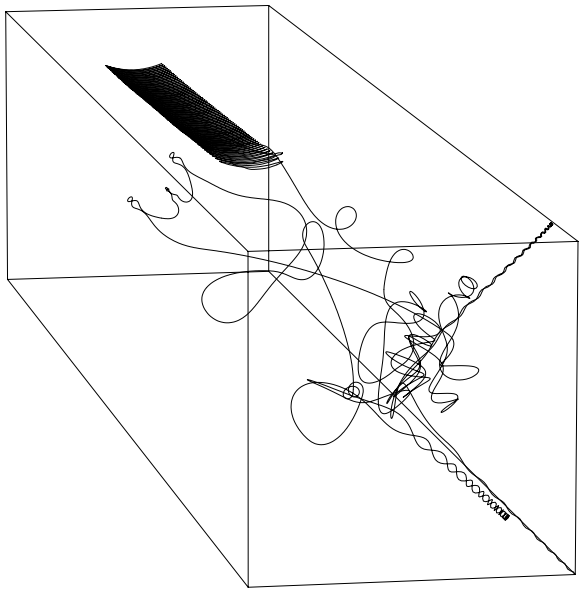

FIG. 1: 3-D plot of an initially deeply trapped electron, which ∇B and $E \times B$ drifts slowly through a magnetic quadrupole, starting from the left. It is accelerated across a drift space, bounces between quadrupoles, then enters the upstream (ion beam frame) quadrupole and is lost radially to the wall.

accelerates electrons backwards across an upstream (beam reference) acceleration gap, or reflects them back to the magnet from an acceleration gap at the downstream end of the magnet. Electrons that gain kinetic energy exceeding the potential trapping energy can be detrapped and deflected to the wall by an upstream magnet, Fig. 1. This is the only mechanism we have identified that will cause trapped electrons to be lost before the end of the beam pulse.

III. HCX FACILITY

Electron cloud experiments in HCX will be primarily performed with four pulsed magnetic quadrupoles. Each magnet has coil lengths of 31 cm, a gradient of up to 16 T/m, a half-lattice length of 52 cm including 4.3 cm for diagnostic access between magnets, and an elliptical bore with 3×5 cm radii at the center [9].

These provide a range of operation from transporting a small diameter beam, with an envelope radius about half that of the walls – minimizing electron and gas generation, to transporting a beam whose envelope approaches or scrapes the walls – maximizing electron

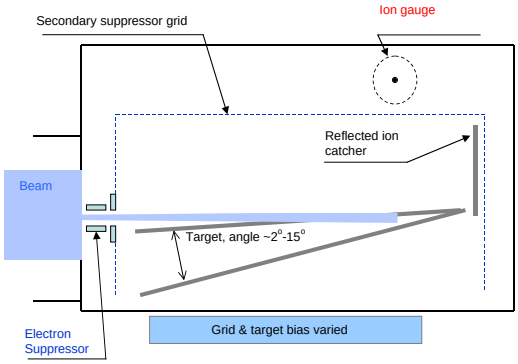

FIG. 2: (Color) The Gas-Electron Source Diagnostic (GESD) measures the number and energy of electrons and gas molecules per incident K^+ ion, and can evaluate mitigation techniques.

and gas generation. To determine limits, we will vary beam operation, until enough beam scrapes the walls to significantly change beam performance or produce electron densities approaching the beam density.

Before the quadrupole magnets are installed, we will begin measurements with the Gas-Electron Source Diagnostic (GESD), Fig. 2. It will be located at the end of the diagnostics tank 1.3 m beyond the end of quadrupole transport. An entrance aperture (0.3 $\times$ 2.5 cm) allows $\sim$0.4% of the beam current into a box where it impacts a target at 75-88° from normal incidence. An ion gauge measures the peak pressure rise, from which we will determine the total gas desorbed from the target.

The target, catcher, and surrounding grid in the GESD can be independently biased relative to the walls, to measure the current and energy of either secondary electrons or low energy secondary ions (up to a few hundred eV), and to determine the beam current to the target. The ion catcher reduces the number of ions scattered into the grid; hence the error in the measured beam current to the target will be small. The energies of desorbed molecules can also be measured by time-of-flight – the wall above the ion gauge can open, increasing the time for gas molecules to reflect back to the gauge to a few hundred microseconds. This will enable us to estimate the time for gas from the wall to reach the beam where it can generate more trapped electrons. Electron (and gas) reduction techniques will be evaluated with the GESD.

FIG. 3: An array of collectors is shown; from left to right is (a) a flush collector, (b) a recessed collector or capacitive probe, (c) a 1-grid, and (d) a 2-grid collector.

We evaluated various diagnostics (Fig. 3) to measure and distinguish secondary electrons due to beam ions impinging on the wall (and to scattered ions resulting from beam ions impinging on the opposite wall), photo-electrons, ions from gas that are expelled with kinetic energy equal to the beam potential at their birth point, and untrapped electrons. A collector at the wall-potential, flush with the surface, measures the net current of all these particles, but can't distinguish between them. A second collector is recessed so that most primary and reflected beam ions can't reach it, but the other particles and electric field can; the difference between the two will be the beam current plus the secondary electron current.

Simple gridded collectors measure the remaining electron sources. A collector, shielded by 1-grid, measures the sum of the current of ions from gas plus untrapped electrons. The grid and collector are recessed so that few scattered ions reach them, since secondary electrons that reach the backside of the grid will be collected. A positive collector bias suppresses photo-electrons. A grounded collector with 2-grids, the second biased to repel electrons, measures the ionization current expelled by the beam. This directly gives the source of ions from ionization of gas. It is closely related to the source of deeply trapped electrons but includes charge exchange as well as ionization of gas. It can also be calibrated to measure the gas pressure within the beam as a function of time.

The escaping electron current will be especially informative at the end of the pulse when the confining potential of the beam decreases with the beam current. Plotting the electron current versus the change in beam potential from the flat-top gives the depth-of-trapping energy distribution for electrons, and the integrated electron charge will give the accumulated trapped electron charge (per unit length and azimuth) at the end of the beam flattop. The difference between the total deeply-trapped electron charge and the integrated ion source term from the 2-grid collector provides an experimental estimate of charge-exchange versus ionization.

Two methods measure the beam potential: (1) Capacitive probes, recessed with no grid,

measure the electric field near the wall (a function of the beam potential). (2) A gridded energy analyzer (GEA) [10] measures the energy distribution of ions (from gas) expelled from the beam (a function of the beam potential distribution). The GEA consists of three grids preceding the collector: a grounded entrance grid, an ion repeller grid, and an electron repeller grid. The novel aspect of this analyzer is biasing the ion repeller grid up to $\sim$5 kV.

In summary, we have listed a variety of simple instruments with which we will begin the quantitative study of the electron-cloud particle balance, the variation of electron-cloud parameters with the fill-factor of the beam in the beam tube, wall conditioning and other mitigation techniques, and – with the use of standard beam diagnostics – the effect of electrons on beam performance in HIF driver-scale beams.

Acknowledgments

We are grateful to Grant Logan for support and encouragement in this work, and to Miguel Furman for stimulating discussions connecting us to the main body of e-cloud work. This work was performed by the University of California Lawrence Livermore National Laboratory under the auspices of the U.S. Department of Energy under contract No. W-7405-ENG-48 and Lawrence Berkeley National Laboratory DE-AC03-76F00098.

---

[1] K. Ohmi, Phys. Rev. Lett. **75**, 1526 (1995).

[2] G. R. L. M. A. Furman, in *Proc. of Internat'l Workshop on Multibunch Instab. in Elec. and Pos. Accelerators* (KEK Proc. 97-17, 1997, Tsukuba, 1997), p. 170.

[3] W. R. Meier, J. J. Barnard, and R. O. Bangerter, Nucl. Instr. and Meth. A **464**, 433 (2001).

[4] P. Seidl (2002), This Symposium.

[5] S. M. Lund (2002), This Symposium.

[6] D. A. Callahan-Miller and M. Tabak, Nucl. Fusion **39**, 883 (1999).

[7] D. E. Baldwin, Rev. Mod. Phys. **49**, 317 (1977).

[8] R. F. Post, Nuclear Fusion **27**, 1579 (1987).

[9] A. Faltens and D. Shuman, Proc. PAC99 p. 3339 (1999).

[10] A. W. Molvik, Rev. Sci. Instrum. **52**, 704 (1981).